RESEARCH ARTICLE

Journal of
RAMAN SPECTROSCOPY WILEY

3D SERS and Raman imaging of protective microcapsules containing bio-active terpenoids

Francesco Cardoni | **Moreno Meneghetti** | **Lucio Litti**

Department of Chemical Sciences, University of Padua, Padua, Italy

Correspondence
Lucio Litti, Department of Chemical Sciences, University of Padua, via Marzolo 1, 35131 Padua, Italy.
Email: lucio.litti@unipd.it

Abstract

Terpenoids play a major role in agriculture, given their fungicidal and herbicidal actions, as well as their favorable toxicological, ecotoxicological, and environmental profiles. Despite all these advantages, terpenoids are reported to be unstable in direct sunlight and atmospheric conditions, so both commercial suppliers and scientific literature foresee their protection by encapsulation. The so-called microcapsules (μCaps) are therefore of high relevance as drug-delivery vectors, but very few techniques focus on their surface as well as on their morphological characterization. Indeed, these aspects are of great importance, given that their surface chemistry governs both their colloidal stability and mechanism of action. Common analysis techniques, such as chromatographic and mass-spectrometric ones, are destructive, require sample preparation, and do not result in the complete morphological characterization of the microcapsules. Micro-Raman spectroscopy, in conjunction with the surface-enhanced Raman spectroscopy (SERS) effect, offers a valuable alternative method of investigation capable of achieving a complete and non-destructive morphological characterization of the terpenoid-encapsulating systems, the dimensions of which fall within the micrometric range. In addition, the SERS effect can be exploited by fabricating the microcapsules with gold nanostars (AuNSs) modified with chitosan and a SERS reporter (Nile Blue A). Thanks to the high contrast provided by the SERS signals of this tag, it was possible to localize and confirm the chitosan in the morphology of the microcapsules. The results of this study shed new light on the possibility of analyzing terpenoid-encapsulating microcapsules and possibly other kinds of encapsulates brought by using Raman spectroscopy and by exploiting the SERS effect.

KEYWORDS

confocal, microcapsule, plasmon, SERS, terpenoids

1 | INTRODUCTION

Terpenes are defined as compounds with molecular structures containing carbon backbones made up of isoprene (2-methylbuta-1,3-diene, C_5H_8) units.[1] Terpenoids are terpene analogs, mostly produced by animals, plants, and microorganisms.[2] They are often the main components of essential oils (EOs) and play functional,

communication, and defense roles.[1,3,4] Given their natural origin, they are also characterized by high biodegradability, in addition to low toxicity toward humans and most animals.[5] Nowadays, terpenoids are of great industrial relevance as, for example, they are used in the food industry as antioxidant and flavoring agents or in phytopharmaceutics because of their antimicrobial, antiviral, as well as herbicide, antifungal, and insect pest repellent properties.[6,7] As a result, many modern pesticide formulations use a mixture of terpenoids as the active ingredient.[5] Nonetheless, terpenoids in agriculture encounter a few severe inconveniences, like their instability to oxidizing agents (oxygen in the air, for instance), light (especially in the UV range), and temperature (both high and low temperatures).[8] These factors ultimately transform terpenoids to alkyl and peroxyl dimers (and possibly to other biologically inactive polymers), through a free radical chain reaction mechanism.[9] For these reasons, encapsulation of terpenoids in agriculture represents an excellent solution for the protection of these active ingredients, indeed increasing their water solubility, and it is widely adopted in commercial products.[10] Encapsulation is defined as a process in which droplets of bioactive oil are surrounded by a surfactant or embedded in a homogeneous or heterogeneous matrix. This results in the production of small capsules with useful properties.[11] The matrix material can either be made up of a synthetic or natural polymer. The most relevant methods to produce terpenoid-encapsulating microcapsules are spray drying, *in situ* polymerization, extrusion, layer-by-layer coating, and coacervation.[12] Coacervation consists of the dissolution of the protective polymer in water (relative concentration ≤10% m/V) in the presence of the dispersed bioactive ingredient. Emulsifiers such as soybean lecithin can be used to stabilize micellar structures prior to the coating process by coacervation, and to achieve electrostatic interactions between the emulsifier and the polymeric coating, ensuring greater stability of microcapsules.[11,13] Recently, natural polymers, such as chitosan, have gained popularity in the field of microencapsulation as coating agents thanks to their natural origin, high stability, and antimicrobial properties.[14] The same principles apply to AMD 10 (*N,N*-dimethylcapramide), used as a green solvent for the production of terpenoid-containing emulsions.[15] Chromatographic and mass-spectrometric techniques are commonly adopted to determine the amount of active principle encapsulated in the microcapsules, the so-called *encapsulation efficiency*.[8] The same approaches are also used to determine the stability of the capsules over time, being able to reveal the presence of degradation products, as well as possible impurities.[16] Nonetheless, these techniques are destructive and do not allow the analysis of the capsules in their native environment, that is, in aqueous dispersion.[8] Micro-Raman spectroscopy, on the other hand, represents a suitable technique to identify the terpenoids within the capsules and to provide a faithful representation of how the sample behaves in its native aqueous environment. The main advantage of using Raman spectroscopy is the possibility of achieving non-destructive analysis with minimal and quick sample preparation. There are only a few examples reporting the use of Raman spectroscopy for the study of the composition and morphology of microcapsules and for the analysis of the encapsulation of bioactive principles.[17,18] However, micro-Raman applied for a deep characterization of the layered structure of microcapsules is still missing. It is, indeed, a challenging task. The core of the capsule is relatively rich in active ingredients and constitutes the largest amount of material in the overall microcapsule. On the other side, the shell is more difficult to reveal, but it is the first part of the formulation to encounter the target of interest, for instance, the pores in a leaf, and to provide protection and stabilization to the capsule itself.[19] Its role is therefore fundamental, as well as the availability of proper methods for its characterization in an aqueous environment. In this study, it is presented the production of typical and of high industrial relevance terpenoid-containing microcapsules, fabricated by coacervation in a protective shell of soybean lecithin and chitosan. Micro-Raman spectroscopy techniques are therefore adopted for in-depth characterization of the formulation, revealing fundamental insights about the chemical and morphological composition of the capsules dispersed in water. Surface-enhanced Raman spectroscopy (SERS) tags, made by functionalized Au nanostars, were also used to enhance the contrast of the outer chitosan layer, composing the shell. The same approach was already demonstrated to be effective in solving the layered structure of a tissue made of labeled cells,[20] while it is herein applied to image the layered structure of a microcapsule. The results presented in this study open a new application of Raman spectroscopy and SERS in the advanced characterization of industrial-relevant microcapsule formulations.

2 | EXPERIMENTAL

2.1 | Materials and instruments

The terpenoids mixture (thymol/geraniol/eugenol, 2:2:1, 40% m/V thymol, 40% m/V geraniol, 20% m/V eugenol), soybean lecithin, $HAuCl_4$, HCl, $AgNO_3$, ascorbic acid, Nile Blue A, and other reagents are purchased by Merck if not differently specified. Chitosan was supplied by Glentham Life Sciences Ltd., and AMD

10 (*N,N*-dimethylcapramide) was obtained from BASF SE. The Agilent Technologies Cary 5000 UV–vis–NIR spectrophotometer was used to acquire all UV–vis spectra presented in this work. The FEI TECNAI G2 transmission electron microscope operating at 100 kV was used to achieve Au nanostars and labeled chitosan imaging. The Renishaw InVia Micro-Raman, equipped with 633 and 785 nm laser excitation, 1200 and 1800 lines/mm grids, and a Leica microscope with objectives from 5 to 100× magnification, was used in all Raman experiments.

2.2 | Synthesis of AuNP by laser ablation

Gold nanoparticles were synthesized starting from bulk gold by the laser ablation synthesis process, following an already reported procedure.[21,22] In summary, a 99.999% pure gold target was fixed at the bottom of a cylindrical glass cell and immersed in a 10 μM NaCl aqueous solution. The target was invested with laser pulses at a fluence of about 1 J/cm^2 using a Q-Smart 450 Nd/YAG laser (6 ns, 1064 nm). The spot diameter on the gold target had a diameter of 1 mm, using a lens of 7.5 cm focal length. The pulse repetition rate was set to 20 Hz. The total ablation time was about 20 min. The concentration of Au atoms within the AuNP colloidal dispersion was evaluated following the work of Polte et al.,[23] namely, using an extinction coefficient of 2.65 L mol^{-1} cm^{-1} at 400 nm, resulting in 1.025 mM. The ablated AuNP extinction spectrum (maximum at 520 nm), as well as electron microscopy characterization (average diameter of 19.5 nm), can be found in Figure S1.

2.3 | Synthesis and characterization of AuNS@CHTS-NBSH

Nile Blue A lipoate (NBSH) and AuNS were obtained following procedures previously reported.[24,25] A total of 5 mL of bi-distilled water, 50 μL of HAuCl$_4$ 30 mM, and 5 μL of HCl 1 M were mixed under vigorous magnetic stirring. Then, 100 μL of AuNP 1.025 mM in [Au], 2.50 μL of AgNO3 10 mM, and 3.50 μL of ascorbic acid 100 mM were added. After 1 min, 1 mL of a 1 g/mL solution of chitosan (dissolved in acidic distilled water, pH = 2.75, as described by Baginskiy et al.)[26] and 250 μL of a 4.5·10^{-7} mM solution of NBSH were added to the solution. The solution was left under vigorous stirring for 1 h. The obtained solution (6.505 mL total volume) was centrifuged for 10 min at 1500 RCF. The supernatant was discarded, and the remaining solution was resuspended with distilled water up to 750 μL. The characterization of the AuNS@CHTS-NBSH system was carried out

by UV–vis absorption spectroscopy, Raman spectroscopy, and transmission electron microscopy (TEM).

2.4 | Preparation of terpenoid-encapsulating formulations

The terpenoid-containing microcapsule formulations (μCap) were produced by mixing 4.0 mL of the terpenoids mixture (40% m/V thymol, 40% m/V geraniol, 20% m/V eugenol), 4.0 mL of AMD 10, 5 mL of a 4% m/V chitosan in water, 2.5 mL of a 10% m/V soybean lecithin in water, and 4.5 mL of distilled water. The mixture was then emulsified with an IKA T25 Ultra Turrax digital disperser for 4 min at 12,000 rpm. "μCap@AuNS" formulation was produced by mixing 4.0 mL of the terpenoids mixture, 4.0 mL of AMD 10, 5 mL of the produced AuNS@CHTS-NBSH solution (4% m/V in chitosan), 2.5 mL of a 10% m/V soybean lecithin in water, and 4.5 mL of distilled water. As for μCap formulation, the obtained μCap@AuNS mixture was emulsified with an IKA T25 Ultra Turrax digital disperser for 4 min at 12,000 rpm. All formulations were stored in the fridge at 4°C.

2.5 | Sample preparation for micro-Raman experiments

Before each Raman measurement, 15 μL of either μCap or μCap@AuNS formulations were deposited over a microscope glass slide, protected by drying with a glass coverslip (0.3 mm thickness), and sealed using a silicon-based glue. The samples were left sitting for 2 h to allow the microcapsules to stabilize and remain stationary for the Raman experiments. An aluminum sheet was used instead of the glass slide whenever 785 nm laser excitation was used for the Raman measure. Single-point Raman spectra were acquired by focusing the excitation laser over the center of the investigated microcapsule. The Leica NPlan L 100x/0.75 objective was used. The laser power on the sample was set to about 3 mW for both the 633 nm and the 785 nm laser lines. For each point, three accumulations were acquired, with an acquisition time of 10 s. 2D Raman maps were acquired using similar acquisition conditions (3 mW laser intensity at 633 and 785 nm, acquisition time of 15 s) but scanning on a defined grid in order to image the full surface at a resolution of 1 μm, both in the *x*- and *y*-axes. Confocal 3D Raman maps were acquired by sampling a volume of about $20 \times 20 \times 20 \ \mu m^3$. The volume was scanned at 1 μm resolution in all the three axes. Laser intensity was set at 0.3 mW at 633 and 785 nm. For each point of the
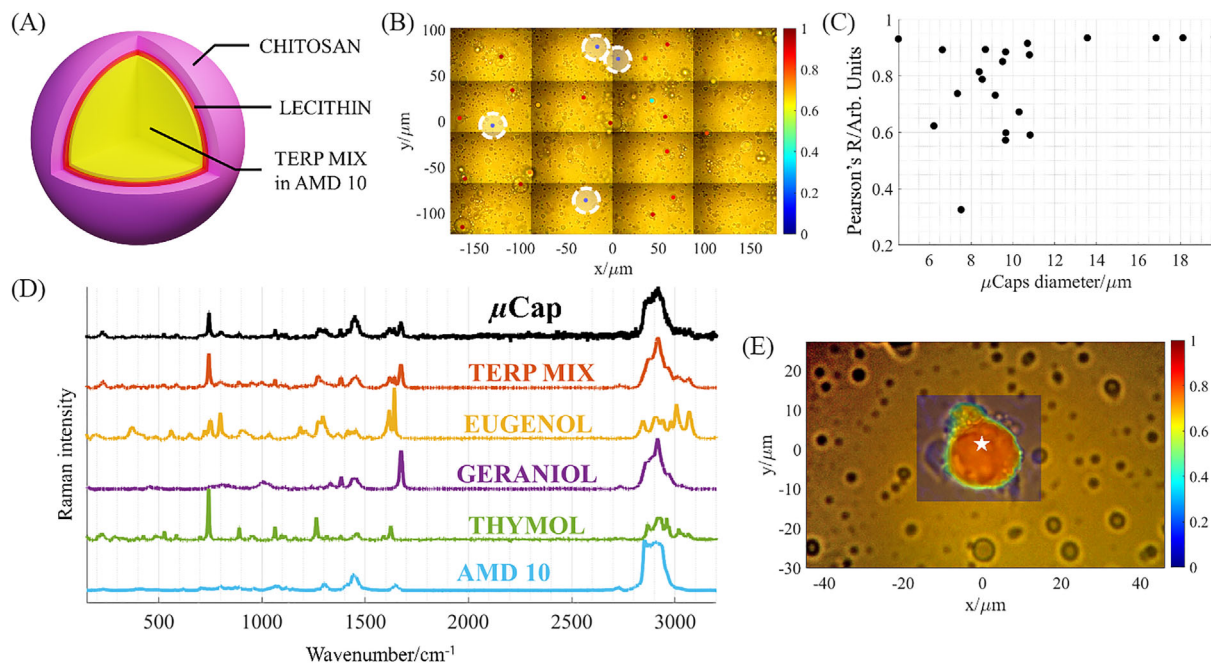
FIGURE 1   (A) Sketched representation of a microcapsule from formulation "µCap". (B) White light image of the microcapsules from formulation "µCap," the false-colored dots represent the correspondence (in terms of Pearson's R coefficient) with the reference Raman spectra of the mixture of terpenoids. The white dashed circles represent the position used to acquire spectra outside any capsule, namely, of the aqueous solution, as reference. (C) Pearson's R coefficient values with respect to the diameter of the analyzed microcapsules. (D) Comparison between the Raman spectrum marked with a white star in (E), "µCap" in black, and the reference Raman spectra of the individual components and of a reference mixture. (E) 2D Raman map of a µCap, acquired using the 633 nm laser excitation. The false colors represent the values of Pearson's R coefficients obtained by comparing the experimental spectra with the reference spectra of the mixture of terpenoids. The white star in the 2D Raman map indicates the acquisition position of the experimental spectrum of (D).

3D grid, the accumulation time was set at 10 s. All the acquired Raman spectra were analyzed by Pearson's correlation coefficient (R) analysis, using built-in Matlab functions, to account for the comparison between the experimental spectra and the reference spectra of pure components and mixtures.

3 | RESULTS AND DISCUSSIONS

The microcapsules (µCap) were obtained by a coacervation approach in which the terpenoids mixture (thymol/geraniol/eugenol, 2:2:1) was diluted in AMD 10 and emulsified in the presence of soybean lecithin and chitosan. The overall layered structure, sketched in Figure 1A, has been investigated because of its morphology by optical microscopy and chemically by micro-Raman spectroscopy.

The micro-Raman analysis at the single µCap level, combined with morphological characterization (Figure 1B), made it possible to correlate the diameter of the µCaps, an average diameter of 10.3 ± 1.8 µm, with the spectral correspondence to the mixture of terpenoids and AMD 10, as reported in Figure 1C. The false colors of

the points in Figure 1B represent the Pearson's correlation (R) with the reference spectrum of the terpenoids and AMD 10 mixture. A red color means R is equal to 1, namely, a perfect correspondence, while the opposite applies to blue colors. The analysis of the correlation between the experimental Raman spectra and the terpenoids and AMD 10 ones allows us to establish a high degree of encapsulation, as both the terpenoids mixture and AMD 10 spectral signatures were always encountered. This indicates that the encapsulation process was effective, as it subtracted the whole amount of the terpenoids mixture from the solution. Even the microcapsule yielding the lowest R-value (R = 0.33, 7.5 µm diameter in Figure 1C) presents important contributions from the terpenoids mixture diagnostic peak, located at 741 cm^{-1} (Figure S2), meaning that it contains the bioactive principles. Capsules with larger diameters seem to possess R values closer to unity and, overall, are less scattered when compared with smaller-diameter capsules. This finding could be attributed to the higher amount of terpenoids mixture present at the cores of these large capsules, which is responsible for the better-resolved Raman spectra. On the other side, smaller capsules possess lower amounts of terpenoids mixture, which results in noisier
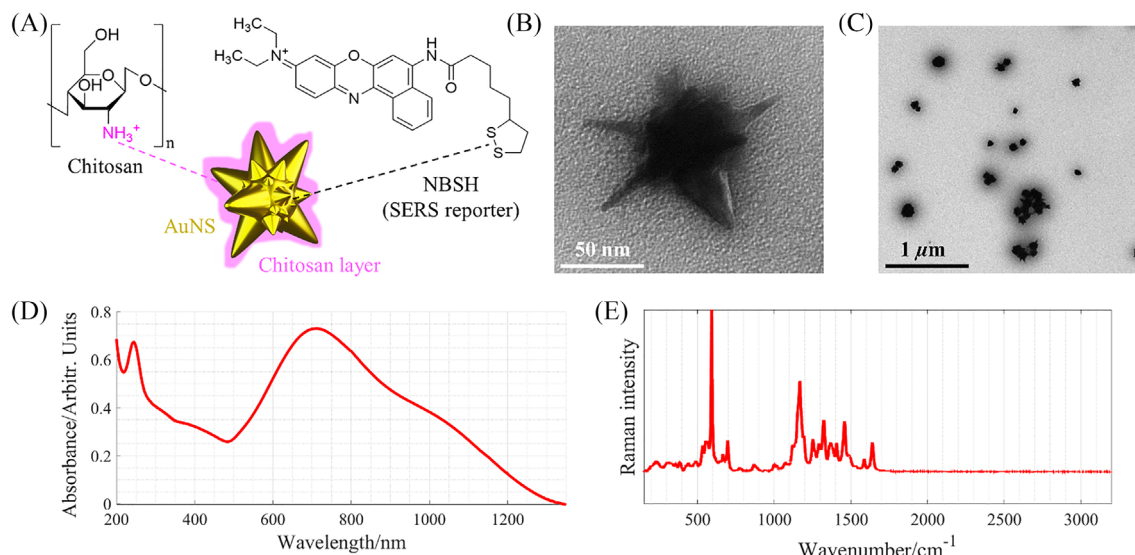
FIGURE 2 (A) Schematic representation of AuNS@CHTS-NBSH structure (not to scale). (B) Transmission electron microscopy (TEM) image of one gold nanostar (AuNS) from AuNS@CHTS-NBSH. (C) TEM image of multiple AuNSs from AuNS@CHTS-NBSH, stained by uranyl acetate. The black halo originating from the staining reveals the presence of chitosan. (D) UV–vis absorption spectrum of the AuNS@CHTS-NBSH solution. (E) Raman spectrum of the AuNS@CHTS-NBSH solution, acquired by using the 785 nm laser excitation. The bands correspond to those of NBSH.

spectra and, ultimately, lower and more scattered R values. In addition, the Raman spectra belonging to the aqueous solution yield the lowest Pearson's correlation coefficient (R) values of the dataset, represented by the blue colors of the respective points in Figure 1B, thus reinforcing the above-stated hypothesis. This is of great interest as, to our knowledge, it constitutes the first attempt to estimate the encapsulation efficiency of the microcapsules in their own environment by a fast and non-destructive technique, indeed correlating the respective capsule dimension. To better understand the differences between the values of Pearson's coefficients of similar Raman spectra acquired at the cores of microcapsules, an analysis was conducted to verify whether the R values depended on the size of the analyzed microcapsule. The obtained results (Figure 1C) disproved the hypothesis, as the trend of R as a function of the diameter of microcapsules is constant to high R values (>0.6) along the entire series. The spectral contributions of terpenoids and AMD 10 are clearly detected in the core of the microcapsules (Figure 1D,E, band assignments in Table S1), while it was not as easy to assign the presence of soybean lecithin and chitosan. Soybean lecithin is supposed to be placed at the oil–water interface, while chitosan is outside the microcapsule cores. It has been reported that a soybean lecithin monolayer possesses a thickness of approximately 30 Å at the oil–water interface,[27] suggesting that the resulting contribution in the Raman spectrum of the whole microcapsule is expected to be minor. Both soybean lecithin and chitosan thus represent a very

limited mass fraction with respect to the overall microcapsule, much richer in the terpenoids mixture. Despite the Raman spectrum of pure chitosan presenting intense and well-resolved peaks (Figure S3), it is supposed that both soybean lecithin and chitosan signals are covered by the signals of terpenoids, present in large excess in the volume sampled by the micro-Raman. Hence, a plasmonic system comprising gold nanostars (AuNSs), chitosan (CHTS), and thiolated Nile Blue A (NBSH) was designed and synthesized to be able to indirectly localize chitosan within the morphology of microcapsules.

Figure 2A shows the schematic representation of the synthesized plasmonic system, herein called AuNS@CHTS-NBSH. The system was extensively characterized using various techniques. TEM images confirm the formation of anisotropic gold tips on the surface of AuNPs used as seeds (Figure 2B), a key feature of AuNSs. Other TEM images, obtained after employing the staining protocol with uranyl acetate, demonstrate the presence of a thick organic layer around the AuNSs (Figure 2C), confirming the successful interaction between AuNSs and chitosan.[28] The average Feret's diameter of AuNS@CHTS-NBSH is 113 ± 5 nm (n = 200, confidence interval of 95%, Figure S4). The UV–vis absorption spectrum reveals the extinction maximum at about 710 nm (Figure 2D). Thiolated Nile Blue A dye (NBSH) was used because of the surface-enhanced resonance Raman scattering effect that takes advantage of the matching between the excitation laser (785 nm), the plasmon band, and the main absorption band of Nile Blue A. For these
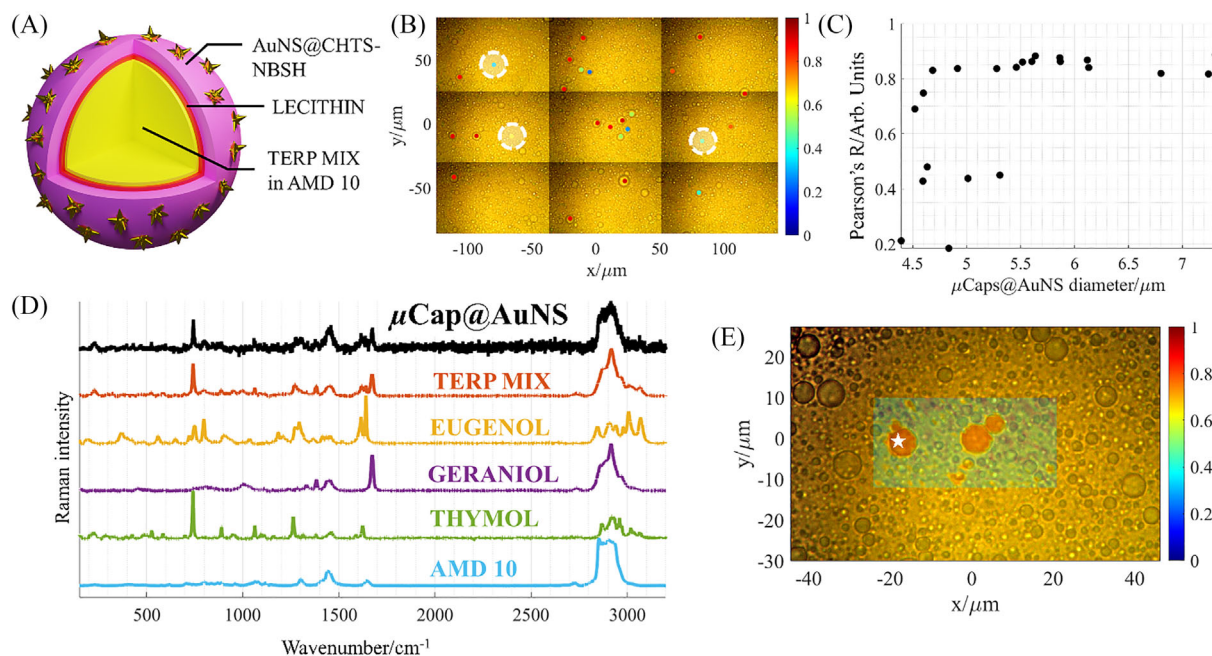
FIGURE 3 (A) Sketched representation of a microcapsule from formulation "μCap@AuNS." (B) White light image of the microcapsules from formulation "μCap@AuNS," the false-colored dots represent the correspondence (in terms of Pearson's R coefficient) with the reference Raman spectra of the mixture of terpenoids and AMD 10. The white dashed circles represent the position used to acquire spectra outside any capsule, namely, of the aqueous solution, as reference. (C) Pearson's R coefficient values in respect to the diameter of the analyzed microcapsules. (D) Comparison between the Raman spectrum marked with a white star in (E), "μCap@AuNS" in black, and the reference Raman spectra of the individual components and of a reference mixture. (E) 2D Raman map of a microcapsule from formulation "μCap@AuNS," acquired by using the 633 nm laser excitation. The false colors represent the values of Pearson's R coefficients obtained by comparing the experimental spectra with the reference spectra of the mixture of terpenoids and AMD 10. The white star in the 2D Raman map indicates the acquisition position of the experimental spectrum of (D).

reasons, Nile Blue A is capable of acting as a bright SERS reporter (Figure 2E). This system was used instead of pure chitosan for the production of microcapsules belonging to the formulation called "μCap@AuNS." The indirect localization of chitosan within the morphology of the microcapsules is now possible by following the diagnostic signals of the SERS reporter (NBSH). The interaction between the microcapsules and AuNS@CHTS-NBSH, with respect to pure chitosan, is assumed unaltered by the fact that the dimensions of AuNS@CHTS-NBSH (~100 nm) are two orders of magnitude smaller than the microcapsules (~10 μm) so that they are sufficiently free to assemble at the interface of the capsules.

The produced microcapsules, belonging to the μCap@AuNS formulation (Figure 3A), have been investigated following the same procedure seen previously for the μCap formulation. The analysis of single-point Raman spectra (Figure 3B) returned an average diameter of 5.5 ± 0.4 μm ($n = 22$, confidence interval of 95%).

As for the μCap formulation, single-point Raman spectra were acquired by focusing the laser beam at the center of the microcapsules belonging to the

μCap@AuNS formulation (Figure 3B). Comparisons with reference spectra made it possible to attribute the experimental Raman signals acquired at the center of the investigated microcapsules ($n = 22$) to the mixture of terpenoids and AMD 10. However, Figure 3C reveals a few microcapsules associated with both small diameter and low Pearson's R with respect to the terpenoids mixture. It would first suggest that these microcapsules have a relatively lower amount of bioactive ingredients inside their core. On the other hand, the R-values distribution is still not dependent on the size of the microcapsules, while the spectra acquired outside any microcapsule in Figure 3B (dashed circles) report higher Pearson's R with respect to Figure 1B. The detailed analysis via 2D Raman map also demonstrates the presence of the terpenoids mixture outside the cores of the microcapsules, although the majority of the active principle is still present within the core of the latter (Figure 3D,E). As a whole, this suggests a lower encapsulation efficiency for the μCap@AuNS with respect to the μCap. As second evidence from Figure 3C, a clear smaller size distribution can be appreciated passing from Figure 1C to Figure 3C, namely, form μCap to
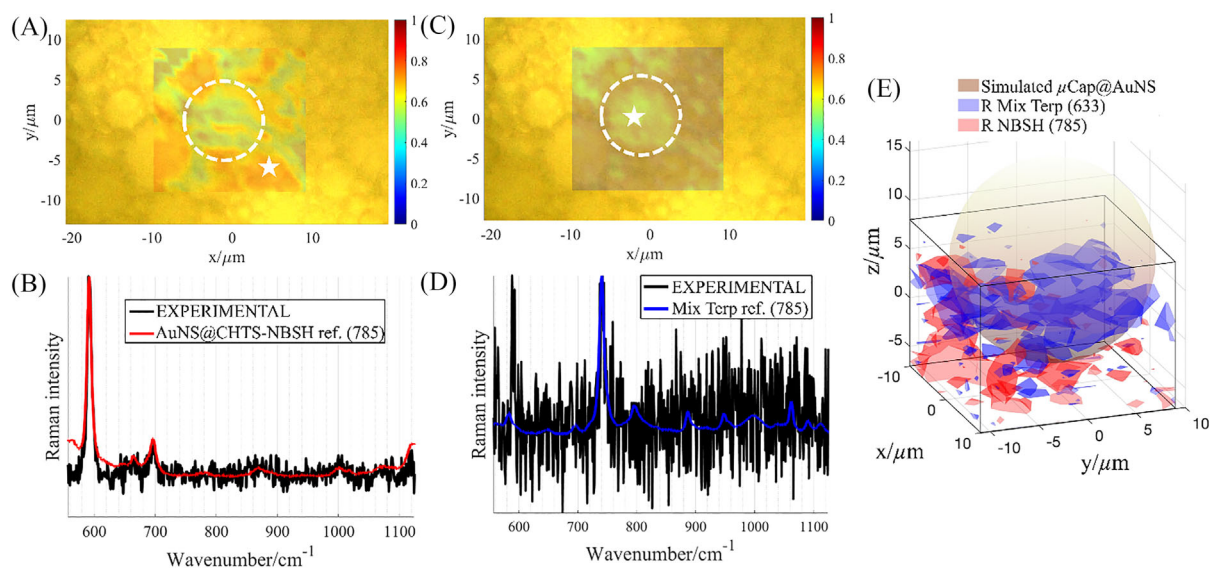
FIGURE 4 (A) 2D Raman map of a microcapsule belonging to the μCap@AuNS formulation, acquired by using the 785 nm laser excitation. The color scale refers the values of the Pearson's correlation coefficient R obtained by comparing the experimental spectra with the reference spectra of AuNS@CHTS-NBSH. The white dashed circle helps with the visualization of the boundaries of the analyzed microcapsule. The white star points to the location of the high R-value experimental spectrum (in black) showed in (B), which is compared with the reference spectrum of AuNS@CHTS-NBSH (in red). (C) 2D Raman map of a microcapsule belonging to the μCap@AuNS formulation, acquired by using the 785 nm laser excitation. The color scale refers the values of the Pearson's correlation coefficient R obtained by comparing the experimental spectra with the reference spectra of the terpenoids mixture (TERP MIX in Figure 1D). The white dashed circle helps with the visualization of the boundaries of the analyzed microcapsule. The white star points to the location of the high R-value experimental spectrum (in black) showed in (D), which is compared with the reference spectrum of the terpenoids mixture (in blue). (E) Combined 3D Raman map of a selected microcapsule from formulation μCap@AuNS, obtained by combining the data from both the 633 and 785 nm laser excitations. The simulated μCap@AuNS (in brown) helps with the visualization of the boundaries of the analyzed microcapsule.

μCap@AuNS formulation, in which pure chitosan is replaced by AuNS@CHTS-NBSH.

The presence of AuNS@CHTS-NBSH within the μCap@AuNS formulation was not clearly evidenced by Raman imaging at 633 nm excitation. It was already discussed that the nanostructures are designed to be better excited at 785 nm, while terpenoids show lower signals at this wavelength with respect to the 633 nm excitation wavelength. Despite Raman imaging, which, due to sharp and resolved vibrational bands, may provide efficient and clear multiplexing,[25,29] the huge excess of some components with respect to others makes it practically ineffective. The usage of dedicated excitations (633 nm for the terpenoids and 785 nm for the AuNS@CHTS-NBSH) solves the issue. 2D Raman imaging of the same microcapsules belonging to the μCap@AuNS formulation was obtained at 785 nm excitation and shown in Figure 4. Two false-colored images were obtained in which experimental spectra were compared with the reference spectrum of AuNS@CHTS-NBSH (Figure 4A,B) and to the reference spectrum of the terpenoids mixture (Figure 4C,D), in all cases under 785 nm excitation. The image in Figure 4C is essentially in agreement with

Figure 3E, namely, the terpenoids signals are localized inside the microcapsule, still with clear traces in the surroundings. The contrast provided by AuNS@CHTS-NBSH in Figure 4A is indeed much higher and allows us to localize the nanostructures preferentially around the microcapsule.

A representative μCap@AuNS microcapsule was also inspected by TEM (Figure S5). Most of the AuNSs (dark spots) are revealed inside the spherical dark shadow, which constitutes the organic component of the microcapsule. This supports the hypothesis according to which the AuNSs are localized preferentially in contact with the external surface of the microcapsules, being intimately linked to the action of chitosan. However, this TEM image only represents a 2D projection of the microcapsule. For this reason, to better understand the three-dimensional morphology of the microspheres, confocal 3D Raman imaging was performed. A representative microcapsule belonging to formulation μCap@AuNS was measured using both the 633 and 785 nm laser lines. The volume inspected considers half of the microcapsule and a portion of the surrounding, namely, a 20 × 20 × 15 μm extension in x, y, and z at a mesh resolution of 1 μm. The

scope is to exploit the different sensitivities of terpenoids mixture and of AuNS@CHTS-NBSH nanostructures at their respective most efficient excitation wavelengths. The results yield a three-dimensional chemical reconstruction of the investigated microcapsule, as depicted in Figure 4E, in which the terpenoids mixture contributions derive from the 633 nm excitation map, while the AuNS@CHTS-NBSH contributions derive from the 785 nm one. A hemisphere is also pictured in the chemical reconstruction of Figure 4E, allowing for a better visualization of the microcapsule volume. The terpenoids signals (in blue) are located inside the core of the investigated microcapsule, while the AuNS@CHTS-NBSH contributions (in red) are mostly outside, at the interface between the oil and water phases. It is also worth noting that the AuNS@CHTS-NBSH signals are not homogeneously distributed around the microcapsule in the sense that they do not offer a complete coverage of its surface, in accordance with the TEM image in Figure S4. 3D confocal Raman maps offered a clear and effective visualization of the three-dimensional morphology of the microcapsules. This technique can thus be used in conjunction with 2D Raman maps and TEM images, which only offer a partial bi-dimensional representation of microcapsules.

4 | CONCLUSIONS

Microcapsules are architectures of great relevance in several fields, as vectors for drug delivery, for instance, intended in both biomedicine and agriculture. Their mechanism of action is often driven by their surface chemistry and interaction with the designated target. Nonetheless, few methods are nowadays adopted for microcapsule characterization in which both chemical and morphological properties are considered. The same applies to the determination of the encapsulation efficiency. In this context, Raman micro-spectroscopy emerges as a valuable technique. It was herein adopted for the structural characterization of a representative formulation containing microcapsules. The encapsulation efficiency was qualitatively evidenced by point-by-point analysis of the microcapsules in their native environment. The layered structure was investigated thanks to the application of chitosan-functionalized SERS tags. In fact, thanks to the utilization of AuNS@CHTS-NBSH in the production of a terpenoids-encapsulating formulation, it has been possible to localize its diagnostic signals outside the microcapsules core, in agreement with the initial hypothesis about the capsule-layered structure. The acquisition of confocal 3D Raman maps helps the understanding of the overall microcapsules morphology.

The results and the approaches herein presented have the great potential of being translated to the analysis of other formulations and would promote micro-Raman spectroscopy for the routine analysis of microcapsule formulations.

CONFLICT OF INTEREST STATEMENT
There are no conflicts of interest to declare.

DATA AVAILABILITY STATEMENT
Raw data are supplied by the authors upon request.

ORCID
Francesco Cardoni https://orcid.org/0009-0003-5308-4439
Moreno Meneghetti https://orcid.org/0000-0003-3355-4811
Lucio Litti https://orcid.org/0000-0001-6247-5456

REFERENCES
[1] C. S. Sell, *A Fragrant Introduction to Terpenoid Chemistry*, The Royal Society of Chemistry, Cambridge **2003**.
[2] S. Perveen, *Terpenes and Terpenoids*, IntechOpen, London **2018**.
[3] A. Masyita, R. Mustika Sari, A. Dwi Astuti, B. Yasir, N. Rahma Rumata, T. Bin Emran, F. Nainu, J. Simal-Gandara, *Food Chem. X* **2022**, *13*, 100217.
[4] A. B. Dehsheikh, M. M. Sourestani, P. B. Dehsheikh, J. Mottaghipisheh, S. Vitalini, M. Iriti, *Mini-Rev. Med. Chem.* **2020**, *20*(11), 958.
[5] M. S. Sankhla, K. Parihar, R. Kumar, D. S. Bhagat, S. S. Sonone, G. K. Singh, V. Nagar, G. Awasthi, C. S. Yadav, *Biointerface Res. Appl. Chem.* **2023**, *13*(2), 114.
[6] M. B. Isman, *Naturally Occurring Bioactive Compounds*, Elsevier, London **2006** 29.
[7] A. K. Pandey, N. Sonker, P. Singh, *J. Food Sci.* **2016**, *81*(4), M928.
[8] C. Turek, F. C. Stintzing, *Compr. Rev. Food Sci. Food Saf.* **2013**, *12*(1), 40.
[9] U. Neuenschwander, I. Hermans, *Phys. Chem. Chem. Phys.* **2010**, *12*(35), 10542.
[10] B. S. Jugreet, S. Suroowan, R. R. K. Rengasamy, M. F. Mahomoodally, *Trends. Food Sci. Technol.* **2020**, *101*, 89.
[11] L. Sagalowicz, M. E. Leser, *Curr. Opin. Colloid Interface Sci.* **2010**, *15*(1–2), 61.
[12] J. Rodríguez, M. J. Martín, M. A. Ruiz, B. Clares, *Food Res. Int.* **2016**, *83*, 41.
[13] S. Ogawa, E. A. Decker, D. J. McClements, *J. Agric. Food Chem.* **2003**, *51*(18), 5522.

[14] M. A. Sani, M. Tavassoli, H. Hamishehkar, D. J. McClements, *Carbohydr. Polym.* **2021**, *255*, 117488.

[15] J. Santos, L. A. Trujillo-Cayado, N. Calero, M. C. Alfaro, J. Muñoz, *J. Ind. Eng. Chem.* **2016**, *36*, 90.

[16] R. P. W. Scott, Essential Oils, in *Encyclopedia of Analytical Science*, Elsevier, London **2005** 554.

[17] M. Mamusa, R. Mastrangelo, T. Glen, S. Murgia, G. Palazzo, J. Smets, P. Baglioni, *Angewandte Chemie - International Edition* **2021**, *60*(44), 23849.

[18] A. Hidalgo, A. Brandolini, V. T. Šaponjac, J. Čanadanović-Brunet, G. Ćetković, *Food Chem.* **2018**, *268*, 40.

[19] M. Mujtaba, K. M. Khawar, M. C. Camara, L. B. Carvalho, L. F. Fraceto, R. E. Morsi, M. Z. Elsabee, M. Kaya, J. Labidi, H. Ullah, D. Wang, *Int. J. Biol. Macromol.* **2020**, *154*, 683.

[20] D. Jimenez de Aberasturi, M. Henriksen-Lacey, L. Litti, J. Langer, L. M. Liz-Marzán, *Adv. Funct. Mater.* **2020**, *30*(14), 1909655.

[21] V. Piotto, L. Litti, M. Meneghetti, *J. Phys. Chem. C* **2020**, *124*(8), 4820.

[22] E. Fazio, B. Gökce, A. De Giacomo, M. Meneghetti, G. Compagnini, M. Tommasini, F. Waag, A. Lucotti, C. G. Zanchi, P. M. Ossi, M. Dell'Aglio, L. D'urso, M. Condorelli, V. Scardaci, F. Biscaglia, L. Litti, M. Gobbo, G. Gallo, M. Santoro, S. Trusso, F. Neri, *Nanomaterials* **2020**, *10*, 2317.

[23] T. Hendel, M. Wuithschick, F. Ketterman, A. Birnbaum, K. Rademann, J. Polte, *Anal. Chem.* **2014**, *86*, 11115.

[24] E. Lenzi, L. Litti, D. Jimenez de Aberasturi, M. Henriksen-Lacey, L. M. Liz-Marzán, *J. Raman Spectrosc.* **2021**, *52*(2), 355.

[25] L. Litti, A. Colusso, M. Pinto, E. Ruli, A. Scarsi, L. Ventura, G. Toffoli, M. Colombatti, G. Fracasso, M. Meneghetti, *Sci. Rep.* **2020**, *10*(1), 15805.

[26] I. Baginskiy, T. C. Lai, L. C. Cheng, Y. C. Chan, K. Y. Yang, R. S. Liu, M. Hsiao, C. H. Chen, S. F. Hu, L. J. Her, D. P. Tsai, *J. Phys. Chem. C* **2013**, *117*(5), 2396.

[27] D. A. Riehm, J. E. Neilsen, G. D. Bothun, V. T. John, S. R. Raghavan, A. V. McCormick, *Mar. Pollut. Bull.* **2015**, *101*(1), 92.

[28] D. Jimenez De Aberasturi, A. B. Serrano-Montes, J. Langer, M. Henriksen-Lacey, W. J. Parak, L. M. Liz-Marzán, *Chem. Mater.* **2016**, *28*(18), 6779.

[29] S. Ricci, M. Buonomo, S. Casalini, S. Bonacchi, M. Meneghetti, L. Litti, *Nanoscale Adv.* **2023**, *5*(7), 1970.

SUPPORTING INFORMATION

Additional supporting information can be found online in the Supporting Information section at the end of this article.